A Proof of Concept of a Structural Supercapacitor Made of Graphene Coated Woven Carbon Fibers: EIS Study and Mechanical Performance

Xoan F. Sánchez-Romate[a,], Antonio Del Bosque[a], Joaquín Artigas-Arnaudas[a], Bianca K. Muñoz[a], María Sánchez[a] and Alejandro Ureña[a]*

[a] Materials Science and Engineering Area, Escuela Superior de Ciencias Experimentales y Tecnología, Universidad Rey Juan Carlos, Calle Tulipán s/n, 28933 Móstoles (Madrid), Spain

*Corresponding author: xoan.fernandez.sanchezromate@urjc.es Tel: +34914884771

ABSTRACT

A multifunctional supercapacitor based on a graphene nanoplatelet (GNP) coated woven carbon fiber (WCF) composite has been manufactured and its electrochemical and mechanical performance has been evaluated. Specific capacitance from voltammetry tests is about three times higher than the non-coated WCFs and several orders of magnitude above neat polymer WCF composites. Furthermore, an electrochemical impedance spectroscopy (EIS) analysis has been carried out in the coated and non-coated WCF capacitors. The equivalent circuit consisted on a series/parallel resistance/constant phase elements. EIS results show that the coated samples have superior capacitor properties, confirmed by chronoamperometry tests. The values of energy and peak power densities were also significantly higher in the coated WCFs, proving higher capabilities as supercapacitors. In addition, mechanical performance of structural supercapacitor is affected by the simultaneous addition of a polymer electrolyte and GNPs, with a reduction of mechanical strength when compared to neat polymer composites. However, and due to the lower viscosity of the electrolyte, there is a higher compaction of the material promoting an increase of WCF volume fraction on the LY-PEGDGE matrix samples, leading to similar values of Young Modulus. Despite the detriment of mechanical properties, they were far above other WCF-based structural supercapacitors. The proof of concept by illuminating a LED was highly successful, proving promising capabilities as structural supercapacitors.

Keywords: graphene nanoplatelets; structural supercapacitor; multifunctional structures; electrochemical analysis; mechanical properties

1. INTRODUCTION

Nowadays, there is an increasing worry about world sustainability and energy demand. More specifically, there are several efforts in reducing CO_2 emissions as they are very harmful for human life and for the proper development of diverse ecosystems *[1,2]*. In this context, there is a continuous interest in investigating alternative sources of energy *[3,4]*, such as solar [5-7]. In fact, the use of universal clean energy by reducing green-house gas emissions is one of the main goals for a sustainable development *[8]*.

In this regard, battery electric vehicles (BEVs) are now attracting the interest of industry as they significantly reduce urban air pollution *[9]*. In fact, BEV market has been doubled in the last years in many developed countries *[10]* as they use cleaner and recyclable energy *[11]*. However, the main issue is the low autonomy in comparison to hybrid and conventional vehicles *[12,13]* so it is necessary to develop novel energy sources or storage devices to make them economically efficient.

Herein, there is an increasing effort in developing multifunctional materials that are able to satisfy the energy demand, as well as to maintain adequate structural performances. In this context, carbon fibre reinforced polymers (CFRPs) seem to be a promising solution as they exhibit some exceptional mechanical and physical properties over conventional alloys. For example, they present much higher specific strength and stiffness and are used for flexural strengthening of bridges *[14,15]*. In aircraft industry, the use of CFRPs is now widely extended and comprises the key material in some major structural parts *[16,17]*. For automotive applications, the use of CFRP materials has been limited to sport or luxury vehicles due to their high cost. However, there are emerging trends in this field in order to produce less expensive fiber reinforced polymers for automotive industry *[18]*.

Furthermore, there is an increasing effort in developing multifunctional supercapacitors for energy storage. A supercapacitor is an intermediate system between electrolytic capacitors and rechargeable batteries. They usually show much higher values of energy per unit volume than electrolytic capacitors and tolerate much more charge and discharge cycles than batteries *[19]*, being a compromise solution between these systems. Here, Electrochemical Double Layer Capacitors (EDLC), based on two electrodes separated by a dielectric media are now of interest, as they show a very high specific power *[20,21]*. In this regard, CFRP-based supercapacitors have gained a great deal of attention within energy storage applications *[22]*. This is explained by the higher surface area of carbon electrodes, which is a crucial point for enhancing the capacitance of electrodes *[23]*. In this context, the manufacturing of three dimensional vertical array scaffolds based on carbon fibers onto conductive fabrics has demonstrated or the use of carbon nanomaterials, such as graphene, have demonstrated excellent capacitance values *[24-26]*.

For these reasons, the interest on surface modified carbon fibers in this application is now gaining attention. For example, the development of graphene modified carbon aerogels have demonstrated good capacitance properties (near 0.3 F/g) without comprising the mechanical performance of CFRP laminates *[27-29]*. Furthermore, Z. Xie et al. observed an important increase in the specific capacitance of supercapacitors with the addition of graphene-based aerogels with different chitosan contents [30]. In addition, it is known that monolayer graphene also improves the absorbance in the infrared spectrum, which can be used for biosensors [31]. Moreover, the synthesis of other nanostructures, such as, CuO and copper cobalt selenide nanowires, have also proved interesting properties for energy storage applications *[32-34]*.

On the other hand, the matrix should give the proper mechanical performances to the composite as well as providing a dielectric media for a sufficient ion mobility. However, these two facts are usually in discordance. Usually, stiffness increases with crosslinking degree whereas ionic transport decreases so most of structural polymers do not allow ionic conductivity *[35]*. Thus, the development of proper structural polymer electrolytes (SPEs) is also of interest. In this regard, several studies developed high-performance epoxy systems with ionic liquid based electrolytes to achieve the desired purpose *[36]*.

Therefore, the present study is focused on the development of a multifunctional supercapacitor based on graphene nanoplatelet (GNP) coated woven carbon fiber composites, by following a facile processing route that would allow to obtain a structural supercapacitor with good energy storage properties without inducing a detrimental of mechanical properties. In this regard, woven glass fiber will be used as separator to promote ionic transport without inducing electrical conductivity. The use of glass fiber is explained because of its good mechanical and insulating properties *[37]*. This separator should be as thinner as possible to improve dielectric and capacitance properties but ensuring the electrical insultation of electrodes *[38-40]*. A high performance epoxy system with an ionic liquid electrolyte will be selected as SPE for the composite structure.

The supercapacitors were manufactured by Vacuum Assited Resin Infusion Moulding (VARIM) due to their cost-efficiency and good final properties. Mechanical performance was evaluated by tensile testing of several samples and energy storage capabilities were evaluated by cyclic voltammetry (CV) tests by comparison to reference CFRP structures as well as by Electrochemical Impedance Spectroscopy (EIS) analysis. Finally, a proof of technology is carried out by lightning a LED using the

fabricated supercapacitor. In this regard, it is important to point out that the main novelty of the present work is the development of a structural supercapacitor with outstanding energy storage capabilities, demonstrated by the proof of concept of lightning a LED.

2. EXPERIMENTAL

2.1. Materials

Woven carbon fiber is a bi-axial 0/90 *HexTow® AS4C 5H 3k* satin weave, supplied by *Hexcel*. Fiber diameter is 6.9 µm, weight/length ratio is 0.2 g/m and a Young Modulus of 231 GPa. Layer thickness is 0.2 mm and specific weight is 280 g/m^2.

Separator is made of glass fiber (GF), *E-Fiberglass Woven Roving*, supplied by *Castro Composites®*. This separator is chosen by its good reinforcement properties. It presents a specific weight of 500 g/m^2 and a humidity content below 0.15 %.

GNPs used in this study are *xGnP® 750 Grade C* ones, supplied by *XGScience®*. They have an average diameter and thickness of 2 µm and 2 nm, respectively. They are selected because of their high specific surface of 750 g/m^2. In addition, a surfactant called *Triton^{TM} X-100*, supplied by *SigmaAldrich®* is used to achieve a better dispersion of GNPs as well as an activating system of WCFs.

Structural resin is an epoxy-based *Araldite® LY 556* with an amino-hardener *XB3473,* supplied by *Huntsman*, in a stoichiometry of 100:23, monomer to hardener. It has a viscosity of 10-12 Pa·s. The structural polymer electrolyte is prepared by a 33.75 wt. % of LY, a 33.75 wt. % of a PEGDGE based resin (60-110 mPa·s viscosity) with a hardener DDS in a proportion 100:35, a 30 wt. % ionic liquid (IL) *EMITSFI* and TiO_2

nanoparticles to improve the ionic transport and structural properties with an average diameter below 25 nm.

2.2. Manufacturing of WCF composites

Four different WCF composites have been manufactured: as received and GNP coated WCF with neat polymer matrix and a solid electrolyte. They are summarized in Table 1.

Table 1: Summary of nomenclature for the different tested supercapacitors.

Manufacturing conditions	Nomenclature
Neat epoxy resin (LY) with uncoated woven carbon fabric	**LY-WCF**
Neat epoxy resin (LY) with GNP coated woven carbon fabric	**LY-GNP-WCF**
Solid electrolyte (LY-PEGDGE-IL) with uncoated woven carbon fabric	**LY-PEGDGE-IL-WCF**
Solid electrolyte (LY-PEGDGE-IL) with GNP coated woven carbon fabric	**LY-PEGDGE-IL-GNP-WCF**

Electrode preparation consisted in a spraying coating of an aqueous solution of GNPs over the WCF, which was previously washed in acetone. This aqueous solution was carried out by the dispersion of GNPs by ultrasonication during 30 min using a *Triton X-100* surfactant to achieve a more stable GNP dispersion, in a similar way than previously stated in other studies *[41,42]*. In this case, the weight contents of GNPs and surfactant were 3 and 5 wt. %, respectively. After spraying, GNP coated WCFs were dried in an oven at 70 ºC for 15 min, prior to resin impregnation. The schematics of spraying process is given in Figure 1 (a).

Simultaneously, polymer electrolyte was prepared by following a three-route step procedure: (1) *Araldite LY 556, PEGDGE* and the ionic liquid *EMITSFI* are mixed and

degasified under vacuum conditions in a magnetic mixer during 1 hour at 80 ºC in order to remove the entrapped air. (2) TiO_2 particles are dispersed in the prepared mixture by means of ultrasonication for 1 hour and finally (3), the nanofilled mixture is degasified for 10 min at 80 ºC under vacuum conditions and the *XB* and *DDS* hardeners are added in 100:23 and 100:35 proportion, respectively.

The manufacturing of structural supercapacitors was carried out by means of Vacuum Assisted Resin Infusion Moulding, VARIM, processing. The supercapacitors were composed by two layers of WCF electrodes with a two-layer GF separator between them. Copper sheets were also attached to each CFRP electrode by using silver ink to ensure a good electrical contact. The set-up of VARIM process and layer sequence is shown in the schematics of Figure 1 (b).

2.3. Electrochemical tests

Cyclic voltammetry tests have been carried out in the four prepared WCF- based composites, by using a potentiostat *AUTOLAB PGSTAT302N* with a software *Nova 2.1*. Working and counter electrodes are connected to each copper sheet, respectively.

Electrochemical response is recorded in a voltage window of -0.5 to 0.5 V at a voltage scan rate of 1 mV/s. Each sample was subjected to 5 consecutive voltammetry cycles in order to determine its specific capacitance. In addition, coated WCF-IL-PEGDGE samples were subjected to CV tests at different scan rates (5, 30, 60 and 100 mV/s).

Chronoamperometry charge-discharge tests and EIS tests were carried out in the LY-PEGDGE based composites to characterize in depth their capacitor capabilities. Chronoamperometry tests were conducted with a voltage step of 1 V applied during 10 s to characterize the initial transient behavior in a similar way than other studies *[37]* and then a discharge window of 1000 s was selected. EIS was performed in 29×19×2

mm^3 samples in a frequency range of 10^5-0.1 Hz. Both tests were also performed in an *AUTOLAB PGSTAT302N* module with a software *Nova 2.1.*

2.4. Mechanical and microstructural characterization

Tensile tests were done in three specimens of each condition accordingly to ASTM D3039 at a test rate of 1 mm/min in a universal tensile machine Zwick with a 100 kN load cell.

Microstructural characterization was done by means of Scanning Electron Microscopy (SEM) using a *S-3400N* apparatus from *Hitachi*. Moreover, for a more detailed analysis of GNP dispersion, Field Emission Gun SEM (FEG-SEM) characterization was carried out by using a *Nova NanoSEM FEI 230* model from *Philips*. In both cases, samples were coated by a thin layer of gold for a proper characterization.

3. RESULTS AND DISCUSSION

3.1 Electrochemical analysis

Figure 2 (a) shows the cyclic voltammetry results for the different tested conditions. Firstly, no significant distortions in the shape of the curve are observed for any condition. This non "duck" shape indicates that there are not redox reactions inside the material *[43]*, meaning also a capacitive behaviour and a charge propagation at the electrode interfaces in a same way as an Electric Double Layer Capacitor (EDLC) *[44]*. Moreover, when comparing CV curves, it is observed that the maximum area corresponds to the LY-PEGDGE-IL-GNP-WCF condition due to the higher surface area of the electrodes explained by the addition of GNPs. From these curves, it is possible to

calculate the specific capacitance, C_{sp}, of the structural supercapacitor by applying the following formula [39]:

$$C_{sp} = \frac{1}{mv(V_c - V_a)} \int_{V_a}^{V_c} IdV \quad (1)$$

Where m is the mass of the electrodes, v the scan velocity rate, fixed at 1 mV/s and $V_c - V_a$ the voltage window, set at 1 V.

Therefore, Table 1 summarizes the C_{sp} for the different conditions. As expected, LY-WCF composites present almost negligible values of capacitance, as seen in the blue curves of Figure 2 (a), especially when comparing to SPE based ones (LY-PEGDGE-IL). Here, GNP anchored WCF materials show a specific capacitance of more than three times over the uncoated WCFs. This is explained by the higher specific area of GNPs, inducing an increase of the specific capacitance over the uncoated WCFs. In addition, Figure 2 (b) summarizes the CV curves at different scan rates. Here, it can be observed that the value of C_{sp} decreases with scan rate. This is a common effect which is explained by the decreasing ion diffusion coefficients at higher scan rates, resulting in an overall detriment *[34,45]*.

For a deeper understanding, Figure 3 summarizes the EIS curves for both the coated and the uncoated LY-PEGDGE composites. It is used to determine the equivalent series resistance (ESR) of the capacitor. Here, it can be observed that EIS curves follow a depressed semicircle at high frequencies followed by an apparent linear slope at low frequencies.

Firstly, the presence of a depressed semicircle indicates that the fitting equivalent circuit of the supercapacitor does not consist in a parallel resistance-capacitance as the resulting curve would be a perfect semicircle. It is correlated to a non-ideal capacitive

behaviour *[46,47]*. For this reason, a constant phase element (CPE) instead of a capacitance is selected.

A CPE is a capacitive element with a constant phase. The impedance is defined by $Z=1/(Q_0(j\omega)^n)$, where Q_0 is a normalization factor and *n* is an exponent indicating the capacitive behaviour of the element. For a value of n=0 it denotes a pure resistive element and n=1 indicates a pure capacitive element. By looking at the measured EIS curves, it can be observed only one depressed semicircle and a linear slope. However, the high frequency region can be composed by the superposition of several depressed semicircles depending on the nature of the system. Furthermore, the linear slope at high frequencies can be also fitted to a depressed semicircle with a high resistance, depending on the diffusion mechanisms *[46]*.

For these reasons, the equivalent circuit used to fit the EIS curves will be based in three parallel resistance-CPE elements, as shown in the schematics of Figure 3 (b) The first one is correlated to the carbon fibre electrodes, the second one corresponds to the double layer capacitor and the third one is related to the GF separator. In addition, the first resistance in series corresponds to the measuring system. Here, the values of the parallel resistances give us an idea of the ionic conductivity capabilities of the electrode and solid electrolyte while the *n* value of the CPE talks about the capacitive or resistive behaviour of each layer.

The adjustment by Nova 2.1 measuring software is represented as solid lines in Figure 3 (a) showing a very good agreement with measured values. In this regard, the values of the resistance and CPEs of the equivalent circuit are summarized in Table 1. Here, several facts can be observed. The first one is that the values of the parallel resistance are significantly higher in case of uncoated WCF capacitor. It is explained by a lower ionic conductivity than the GNP coated supercapacitor, explained by the higher specific

surface of the coated fibres, which was reflected in a superior specific capacitance, as stated before. Moreover, it can be observed that the CPE presents a mostly capacitive behaviour in the electrode and double layer regions, as expected whereas the GF separator acts as a mostly resistive element with a very high parallel resistance.

Furthermore, to get a deeper knowledge of supercapacitor characteristics; energy and power density can be calculated attending the chronoamperometry tests.

In this context, Figure 4 summarizes the charge and discharge curves during chronoamperometry for the different structural supercapacitors. Here, the results of neat epoxy systems are not shown as they do not have any capacitor capabilities, as seen in the CV tests. From these tests, it is possible to estimate the energy and peak power densities by using the following formula from N. Shirshova et al. *[37]*:

$$E = \frac{1}{2} C_{sp} {U_{int}}^2 \qquad P = \frac{{U_{int}}^2}{4R_s} \tag{2}$$

Where C_{sp} is the specific capacitance, previously calculated and $U_{int} = \frac{R_p}{R_P + R_s} U_{applied}$ is the internal voltage of the capacitor. Here $U_{applied}$ is the applied voltage during the chronoamperometry tests and R_s is the resistance of the electrode, given by the value of the parallel resistance of the electrode region and R_p the resistance of the double layer region.

The values of energy and peak power densities are also summarized in Table 1. Here, it can be stated that both energy and peak power densities of uncoated WCFs are significantly lower when comparing to GNP coated ones, so the last one demonstrates superior capacitor capabilities. Moreover, although peak power density is quite low, the values of specific capacitance and energy densities are significantly higher than other found in the literature for WCF based structural supercapacitors *[37]*.

Table 1: Electrochemical values of structural supercapacitors (samples with neat epoxy resin were not subjected to EIS and charge-discharge chronoamperometry tests).

		Electrode	Double-layer	GF separator		
Condition	$C_{sp}(mF/g)$	$R(\Omega g)/CPE(n)$	$R(\Omega g)/CPE(n)$	$R(\Omega g)/CPE(n)$	**E (mWh/kg)**	**P (W/kg)**
LY-WCF	$2.9 \cdot 10^{-7}$	-	-	-	-	-
LY-GNP-WCF	$2.95 \cdot 10^{-7}$	-	-	-	-	-
LY-PEGDGE-IL-WCF	3.07	435/0.86	510/0.71	$1.1 \cdot 10^{12}$/0.3	0.89	0.168
LY-PEGDGE-IL-GNP-WCF	9.6	116/0.87	309/0.797	$1.1 \cdot 10^{12}$/0.46	2.86	1.139

3.2 Mechanical performance

Figure 5 shows the stress-strain curves for the different conditions tested. It is observed that Young Modulus barely changes with the GNP addition onto WCF as well as by using the SPE or the neat epoxy matrix. On one side, these results indicate that the GNP coating does not significantly affect the load transferring between WCF and SPE. However, at first sight, GNP addition should enhance the mechanical properties of the bare WCF composites due to the increase of interfacial adhesions between the carbon fiber and the polymer matrix *[29,34]* as their higher specific area. In fact, a slight increase of Young's Modulus and tensile strength is observed when comparing the pristine polymer matrix when coating WCF with GNPs, where no lack of interfacial adhesion is observed between the fiber and the matrix, as observed in the SEM micrographs of Figure 6 (a) and (b). However, in the case of polymer electrolyte matrix,

there is a decrease of tensile strength of about 10-15 %. This is due to a poor interfacial adhesion between WCF and polymer matrix that can be observed in several areas (Figures 6 (c) and (d)). This lack of adhesion can be explained attending the low viscosity of the polymer electrolyte that, according to Darcy's Law, leads to a higher velocity of fluid, inducing a dragging effect over the GNPs. In this context, FEG-SEM images of fracture surfaces of Figure 7 show an irregular distribution of GNPs in case of LY-PEGDGE-IL samples, promoting areas without GNP coating (Figure 7 (a)) and others with a high aggregation of nanoparticles (Figure 7 (b)). This dragging effect could cause the reaggregation of GNPs, promoting this lack of interfacial adhesion observed as well as the presence of GNP rich areas that could lead to a reduction of mechanical properties *[48,49]*. This dragging effect could also explain the lower values of R_p previously observed, as it would induce areas with much higher amount of nanoparticles acting as electrical connections between electrodes and, thus, reducing the electrical resistance between electrodes. However, this dragging effect is not so prevalent in the pristine matrix, as observed in a much more regular GNP distribution over the WCF surface (Figures 7 (c) and (d)). This is explained because of the viscosity of neat resin LY that is much higher than LY-PEGDGE-IL and, therefore, the velocity during infusion is much lower, leading to a much better interfacial adhesion between the polymer matrix and WCFs as there is not prevalent dragging effect of the GNPs, similar to that observed for the uncoated WCFs.

Moreover, Young's Modulus of composites does not significantly changes when comparing the neat epoxy system and SPE. These results can be surprising at first sight as the mechanical performance and, specially, the stiffness of the LY-PEGDGE is much lower than neat epoxy due to a drastic reduction of the cross-linking degree *[50,51]*. However, the thickness of the samples with electrolyte is much lower, as summarized in

Table 2. As the amount of WCF and GF separator is kept constant, it induces an increase of the volume fraction of WCF over the neat polymer composites as can be observed in the values estimated from the specific weight and layer thickness. This increase in the volume fraction can be explained by a higher compaction at vacuum conditions during manufacturing, due to the lower viscosity of the resin, which induces a higher resin bleeding during the cure cycle.

Table 2: Mechanical properties and thickness of the different specimens.

Condition	Young Modulus (GPa)	Tensile Strength (MPa)	Thickness (mm)	V_f
LY-WCF	24.1 ± 0.9	426 ± 29	1.20 ± 0.04	0.338
LY-GNP-WCF	23.8 ± 1.5	457 ± 3	1.18 ± 0.04	0.339
LY-PEGDGE-IL-WCF	23.7 ± 0.3	337 ± 21	0.84 ± 0.03	0.476
LY-PEGDGE-IL-GNP-WCF	24.0 ± 1.6	294 ± 9	0.86 ± 0.03	0.465

When comparing the mechanical properties of the developed structural supercapacitor with others found in the literature, a good overall performance is observed. More specifically, it shows very good mechanical properties (Young Modulus's increasing from 18 to 24 GPa) than some developed supercapacitors based on activated carbon fibers *[37]* and significantly superior when comparing to another kind of supercapacitors based on CNT coated stainless steel electrodes, where a Young Modulus of 5 GPa and a tensile strength of 85 MPa were achieved *[52]*, far below the values obtained in the present study.

Therefore, from the mechanical point of view, it can be said that the developed GNP coated WCF based supercapacitors have a good potential and could be used in structural applications without significantly compromising the overall mechanical performance.

3.3 Proof of concept

A proof of concept in the GNP coated structural capacitor (LY-PEGDGE-IL-GNP-WCF) was carried out by doing a simple electrical arrangement. The aim was to illuminate a LED as long as possible. To achieve this purpose, the structural supercapacitor was charged by a 4.5 V for 2 hours, then disconnected from the battery (Figure 8 (a)) and finally connected to a LED. The measured voltage of the device was about 1.8 V and the LED was continuously illuminated for more than an hour (Figures 8 (b) and (c)) as can be seen in the Supplementary Video File. During this period, the voltage generated by the device fell from 1.85 to 1.75 V, demonstrating very high power and energy densities. At the last stages of the test, the luminescence of the LED decreases, as observed in Figure 8 (c).

Additionally, the same tests were carried out in the non-coated WCF/LY-PEGDGE-IL composites. Here, the measured voltage after the disconnection from the battery ranges from 0.3 V at the beginning to 0.1 V after 10 min. This voltage was not enough to illuminate the LED. As expected, the neat polymer-based composites did not show any energy storage capability, as they do not allow ionic transport.

Supplementary Video File

Therefore, the results of the proof of concept test revealed a higher potential for energy storage purposes of the proposed GNP coated structural supercapacitors.

4. CONCLUSIONS

The electrochemical and mechanical properties of woven carbon fiber (WCF) composite structural supercapacitors has been investigated. To achieve this purpose, several combinations of non-coated and graphene nanoplatelet (GNP) coated WCF with neat epoxy and polymer electrolyte have been tested.

It has been observed that the neat epoxy system presents negligible values of capacitance as the polymer does not allow ionic transport. When comparing the two systems using a structural polymer electrolyte it has been noticed that the GNP coated WCF based one shows capacitance values three times higher than the non-coated due to the increase of specific surface area induced by the nanoparticles. EIS analysis show a higher capacitive behaviour of the coated WCF capacitor with a closer oppressed semicircle. In this regard, the equivalent circuit shows a series-parallel R/CPE elements with higher resistance values in case of uncoated WCF capacitors. The values of energy and peak power density are also significantly higher in the coated specimens and comparable to other studies.

Mechanical properties are affected by the addition of a polymer electrolyte as well as by GNPs. In the first case, the lower viscosity of the structural electrolyte leads to a higher compaction during curing and thus, a higher volume fraction of WCFs. Simultaneously, the lower stiffness of the electrolyte could promote a detrimental of mechanical properties. In the second case, GNPs promote a reduction on mechanical strength due to the dragging effect during VARIM process. It can induce a reaggregation of nanoparticles, acting as stress concentrators. However, the mechanical performance is better than most of WCF based structural supercapacitors found in the literature.

Finally, a proof of concept has been carried out by using a LED. Excellent supercapacitor properties have been proved by continuously illuminating the LED for more than 1 hour after charging the WCF structure with a 4.5 V battery. Therefore, a good potential and applicability as structural supercapacitors have been demonstrated. In this regard, this system would be, thus, suitable for energy storage applications (i.e. a possible future application in electric vehicles). However, a deeper analysis focused on EIS performance with varying the WCF coating method as well as the solid electrolyte would be needed in order to develop a more efficient structural supercapacitor.

ACKNOWLEDGEMENTS

This work was supported by the Ministerio de Economía y Competitividad of Spanish Government [Project MAT2016-78825-C2-1-R].

REFERENCES

[1] I. Nagelkerken, S.D. Connell, Global alteration of ocean ecosystem functioning due to increasing human CO2 emissions, Proc. Natl. Acad. Sci. U. S. A. 112 (2015) 13272-13277.

[2] G.H. Rau, J.R. Baird, Negative-CO2-emissions ocean thermal energy conversion, Renewable and Sustainable Energy Reviews 95 (2018) 265-272.

[3] R. Madlener, Y. Sunak, Impacts of urbanization on urban structures and energy demand: What can we learn for urban energy planning and urbanization management? Sustainable Cities and Society 1 (2011) 45-53.

[4] K. Hansen, B.V. Mathiesen, I.R. Skov, Full energy system transition towards 100% renewable energy in Germany in 2050, Renewable and Sustainable Energy Reviews 102 (2019) 1-13.

[5] Z. Yi, J. Li, J. Lin, F. Qin, X. Chen, W. Yao, et al., Broadband polarization-insensitive and wide-angle solar energy absorber based on tungsten ring-disc array, Nanoscale (2020).

[6] F. Zhao, X. Chen, Z. Yi, F. Qin, Y. Tang, W. Yao, et al., Study on the solar energy absorption of hybrid solar cells with trapezoid-pyramidal structure based PEDOT: PSS/c-Ge, Solar Energy 204 (2020) 635-643.

[7] P. Yu, H. Yang, X. Chen, Z. Yi, W. Yao, J. Chen, et al., Ultra-wideband solar absorber based on refractory titanium metal, Renewable Energy (2020).

[8] D. Griggs, M. Stafford-Smith, O. Gaffney, J. Rockström, M.C. Öhman, P. Shyamsundar, et al., Policy: Sustainable development goals for people and planet, Nature 495 (2013) 305.

[9] X. Ou, X. Zhang, X. Zhang, Q. Zhang, Life cycle GHG of NG-based fuel and electric vehicle in China, Energies 6 (2013) 2644-2662.

[10] J. Du, X. Meng, J. Li, X. Wu, Z. Song, M. Ouyang, Insights into the characteristics of technologies and industrialization for plug-in electric cars in China, Energy 164 (2018) 910-924.

[11] T. Wilberforce, Z. El-Hassan, F.N. Khatib, A. Al Makky, A. Baroutaji, J.G. Carton, et al., Developments of electric cars and fuel cell hydrogen electric cars, International Journal of Hydrogen Energy 42 (2017) 25695-25734.

[12] J. Madslien, The future of electric motoring, BBC News, dated on 16 (2009) 2009.

[13] F. Zhang, P. Cooke, The green vehicle trend: electric, plug-in hybrid or hydrogen fuel cell, Dynamics of Institutions and Markets in Europe (2009).

[14] D. Schnerch, S. Rizkalla, Flexural strengthening of steel bridges with high modulus CFRP strips, J. Bridge Eng. 13 (2008) 192-201.

[15] T.C. Miller, M.J. Chajes, D.R. Mertz, J.N. Hastings, Strengthening of a steel bridge girder using CFRP plates, J. Bridge Eng. 6 (2001) 514-522.

[16] B. Chatterjee, S. Bhowmik, Chapter 9 - Evolution of material selection in commercial aviation industry—a review, (2019) 199-219.

[17] M. Arena, M. Viscardi, G. Barra, L. Vertuccio, L. Guadagno, Multifunctional performance of a nano-modified fiber reinforced composite aeronautical panel, Materials 12 (2019) 869.

[18] M. Pervaiz, S. Panthapulakkal, K. Birat, M. Sain, J. Tjong, Emerging trends in automotive lightweighting through novel composite materials, Materials sciences and Applications 7 (2016) 26.

[19] Z. Bi, T. Kan, C.C. Mi, Y. Zhang, Z. Zhao, G.A. Keoleian, A review of wireless power transfer for electric vehicles: Prospects to enhance sustainable mobility, Appl. Energy 179 (2016) 413-425.

[20] J.R. Miller, P. Simon, Materials science. Electrochemical capacitors for energy management, Science 321 (2008) 651-652.

[21] Z.S. Iro, C. Subramani, S. Dash, A brief review on electrode materials for supercapacitor, Int.J.Electrochem.Sci 11 (2016) 10628-10643.

[22] L.E. Asp, E.S. Greenhalgh, Structural power composites, Composites Science and Technology 101 (2014) 41-61.

[23] R. Kötz, M. Carlen, Principles and applications of electrochemical capacitors, Electrochimica Acta 45 (2000) 2483-2498.

[24] S. Bellani, E. Petroni, Del Rio Castillo, Antonio Esau, N. Curreli, B. Martín-García, R. Oropesa-Nuñez, et al., Scalable Production of Graphene Inks via Wet-Jet Milling Exfoliation for Screen-Printed Micro-Supercapacitors, Advanced Functional Materials 29 (2019) 1807659.

[25] X. Li, J. Wang, K. Wang, J. Yao, H. Bian, K. Song, et al., Three-dimensional stretchable fabric-based electrode for supercapacitors prepared by electrostatic flocking, Chemical Engineering Journal 390 (2020) 124442.

[26] D. Ou, J. Liu, J. Yan, Q. Qin, J. Xu, Y. Wu, Construction of three-dimensional graphene like carbon on carbon fibers and loading of polyaniline for high performance asymmetric supercapacitor, Electrochimica Acta 335 (2020) 135679.

[27] H. Qian, A.R. Kucernak, E.S. Greenhalgh, A. Bismarck, M.S. Shaffer, Multifunctional structural supercapacitor composites based on carbon aerogel modified high performance carbon fiber fabric, ACS applied materials & interfaces 5 (2013) 6113-6122.

[28] E. Greenhalgh, J. Ankersen, L. Asp, A. Bismarck, Q. Fontana, M. Houlle, et al., Mechanical, electrical and microstructural characterisation of multifunctional structural power composites, J. Composite Mater. 49 (2015) 1823-1834.

[29] A. Javaid, M. Irfan, Multifunctional structural supercapacitors based on graphene nanoplatelets/carbon aerogel composite coated carbon fiber electrodes, Materials Research Express 6 (2018) 016310.

[30] Z. Xie, J. Zhu, Y. Bi, H. Ren, X. Chen, H. Yu, Nitrogen-Doped Porous Graphene-Based Aerogels toward Efficient Heavy Metal Ion Adsorption and Supercapacitor Applications, physica status solidi (RRL)–Rapid Research Letters 14 (2020) 1900534.

[31] C. Cen, Z. Chen, D. Xu, L. Jiang, X. Chen, Z. Yi, et al., High quality factor, high sensitivity metamaterial graphene—perfect absorber based on critical coupling theory and impedance matching, Nanomaterials 10 (2020) 95.

[32] B.K. Deka, A. Hazarika, J. Kim, Y. Park, H.W. Park, Multifunctional CuO nanowire embodied structural supercapacitor based on woven carbon fiber/ionic liquid–polyester resin, Composites Part A: Applied Science and Manufacturing 87 (2016) 256-262.

[33] L. Lim, Y. Liu, W. Liu, R. Tjandra, L. Rasenthiram, Z. Chen, et al., All-in-one graphene based composite fiber: toward wearable supercapacitor, ACS applied materials & interfaces 9 (2017) 39576-39583.

[34] B.K. Deka, A. Hazarika, J. Kim, N. Kim, H.E. Jeong, Y. Park, et al., Bimetallic copper cobalt selenide nanowire-anchored woven carbon fiber-based structural supercapacitors, Chem. Eng. J. 355 (2019) 551-559.

[35] C. González, J. Vilatela, J. Molina-Aldareguía, C. Lopes, J. LLorca, Structural composites for multifunctional applications: current challenges and future trends, Progress in Materials Science 89 (2017) 194-251.

[36] N. Shirshova, A. Bismarck, E.S. Greenhalgh, P. Johansson, G. Kalinka, M.J. Marczewski, et al., Composition as a means to control morphology and properties of epoxy based dual-phase structural electrolytes, The Journal of Physical Chemistry C 118 (2014) 28377-28387.

[37] N. Shirshova, H. Qian, M.S. Shaffer, J.H. Steinke, E.S. Greenhalgh, P.T. Curtis, et al., Structural composite supercapacitors, Composites Part A: Applied Science and Manufacturing 46 (2013) 96-107.

[38] T. Carlson, D. Ordéus, M. Wysocki, L.E. Asp, Structural capacitor materials made from carbon fibre epoxy composites, Composites Sci. Technol. 70 (2010) 1135-1140.

[39] B.K. Deka, A. Hazarika, J. Kim, Y. Park, H.W. Park, Recent development and challenges of multifunctional structural supercapacitors for automotive industries, Int. J. Energy Res. 41 (2017) 1397-1411.

[40] K. Chan, B. Jia, H. Lin, N. Hameed, J. Lee, K. Lau, A critical review on multifunctional composites as structural capacitors for energy storage, Composite Structures 188 (2018) 126-142.

[41] X.X. Fernández Sánchez-Romate, J. Molinero, A. Jiménez-Suárez, M. Sánchez, A. Güemes, A. Ureña, Carbon Nanotube Doped Adhesive Films for Detecting Crack Propagation on Bonded Joints: A Deeper Understanding of Anomalous Behaviors, ACS applied materials & interfaces (2017).

[42] X.F. Sánchez-Romate, R. Moriche, A. Jiménez-Suárez, M. Sánchez, A. Güemes, A. Ureña, An approach using highly sensitive carbon nanotube adhesive films for crack growth detection under flexural load in composite structures, Composite Structures 224 (2019) 111087.

[43] N. Elgrishi, K.J. Rountree, B.D. McCarthy, E.S. Rountree, T.T. Eisenhart, J.L. Dempsey, A practical beginner's guide to cyclic voltammetry, J. Chem. Educ. 95 (2017) 197-206.

[44] M. Cakici, R.R. Kakarla, F. Alonso-Marroquin, Advanced electrochemical energy storage supercapacitors based on the flexible carbon fiber fabric-coated with uniform coral-like MnO2 structured electrodes, Chemical Engineering Journal 309 (2017) 151-158.

[45] H. Qian, A. Bismarck, E.S. Greenhalgh, M.S. Shaffer, Carbon nanotube grafted carbon fibres: a study of wetting and fibre fragmentation, Composites Part A: Applied science and manufacturing 41 (2010) 1107-1114.

[46] N.A. Cañas, K. Hirose, B. Pascucci, N. Wagner, K.A. Friedrich, R. Hiesgen, Investigations of lithium–sulfur batteries using electrochemical impedance spectroscopy, Electrochim. Acta 97 (2013) 42-51.

[47] M. Frankenberger, M. Singh, A. Dinter, K. Pettinger, EIS Study on the Electrode-Separator Interface Lamination, Batteries 5 (2019) 71.

[48] X. Wang, L. Song, W. Pornwannchai, Y. Hu, B. Kandola, The effect of graphene presence in flame retarded epoxy resin matrix on the mechanical and flammability properties of glass fiber-reinforced composites, Composites Part A: Applied Science and Manufacturing 53 (2013) 88-96.

[49] R. Moriche, M. Sánchez, A. Jiménez-Suárez, S.G. Prolongo, A. Ureña, Electrically conductive functionalized-GNP/epoxy based composites: From nanocomposite to multiscale glass fibre composite material, Composites Part B: Engineering 98 (2016) 49-55.

[50] H. Ben youcef, O. Garcia-Calvo, N. Lago, S. Devaraj, M. Armand, Cross-Linked Solid Polymer Electrolyte for All-Solid-State Rechargeable Lithium Batteries, Electrochimica Acta 220 (2016) 587-594.

[51] Y. Liu, D. Lin, P.Y. Yuen, K. Liu, J. Xie, R.H. Dauskardt, et al., An artificial solid electrolyte interphase with high Li-ion conductivity, mechanical strength, and flexibility for stable lithium metal anodes, Adv Mater 29 (2017) 1605531.

[52] N. Muralidharan, E. Teblum, A.S. Westover, D. Schauben, A. Itzhak, M. Muallem, et al., Carbon Nanotube Reinforced Structural Composite Supercapacitor, Scientific reports 8 (2018) 17662.

LIST OF FIGURES

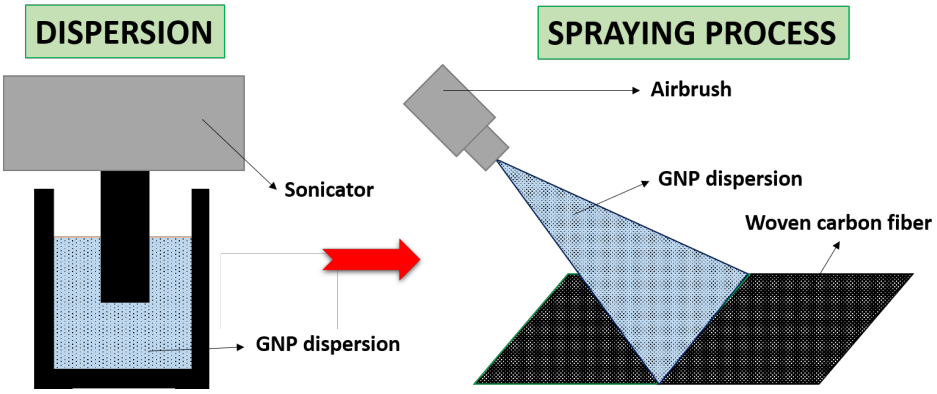

(a)

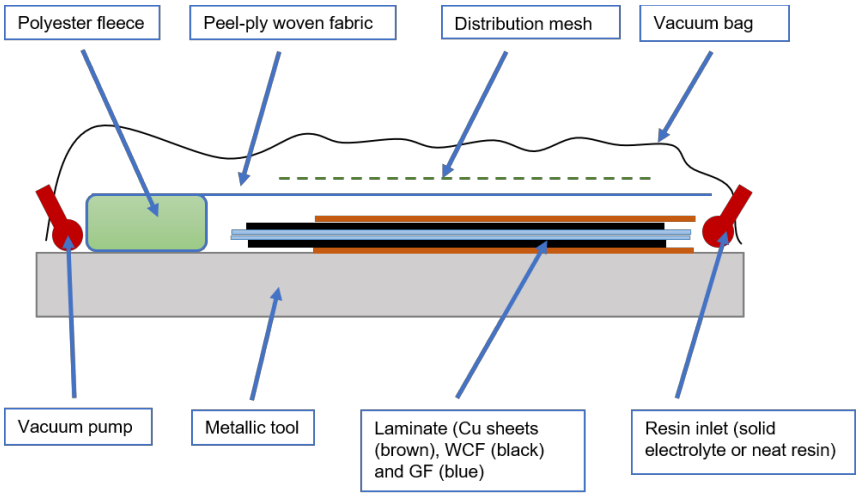

(b)

Figure 1: Schematics of (a) GNP dispersion and spraying over the WCF surface and (b) vacuum bag during VARIM process.

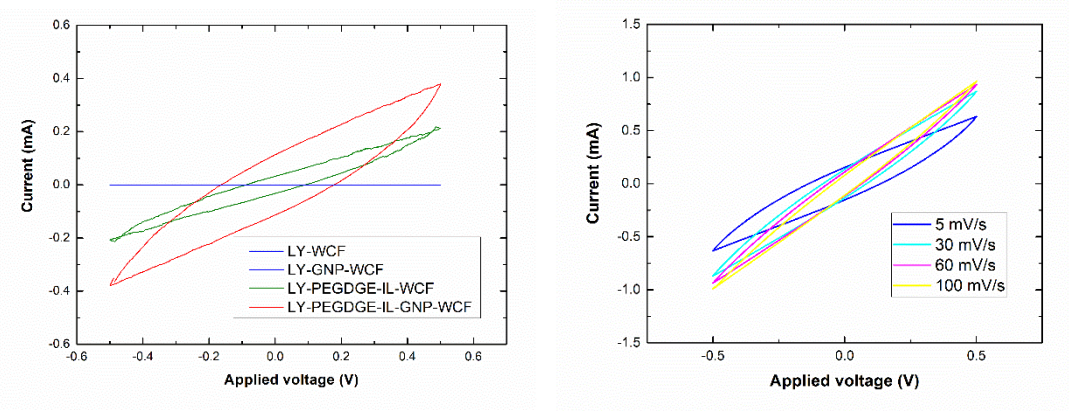

(a) (b)

Figure 2: Cyclic voltammetry of WCF based composites showing (a) the behaviour of the different composites at 1 mV/s and (b) the behaviour of LY-PEGDGE-IL-GNP-WCF at different scan rates.

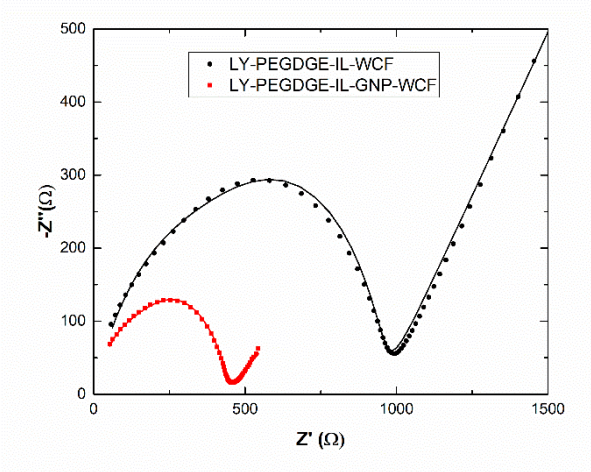

(a)

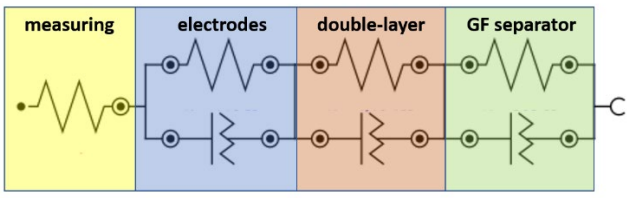

(b)

Figure 3: (a) EIS curves for the uncoated and coated LY-PEGDGE-IL-WF samples where solid lines denotes the estimations by using (b) the equivalent circuit.

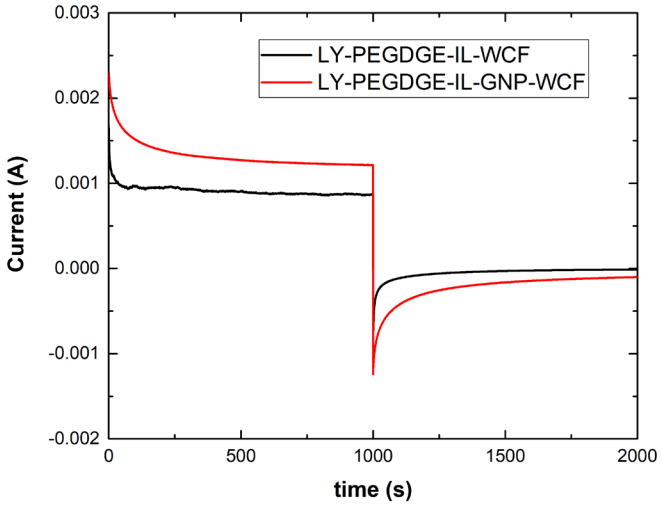

Figure 4: Charge-discharge curves of chronoamperometry tests.

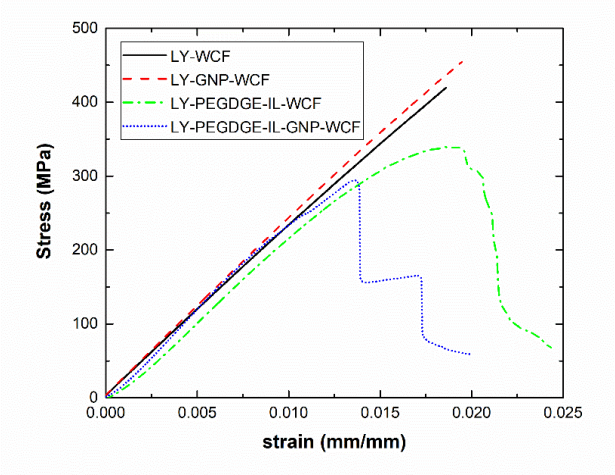

Figure 5: Stress-strain curves for the different WCF based composites.

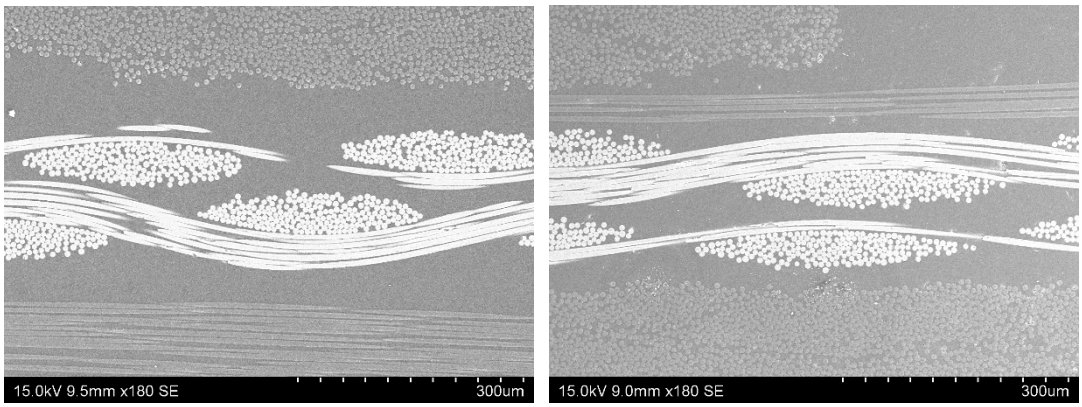

(a) (b)

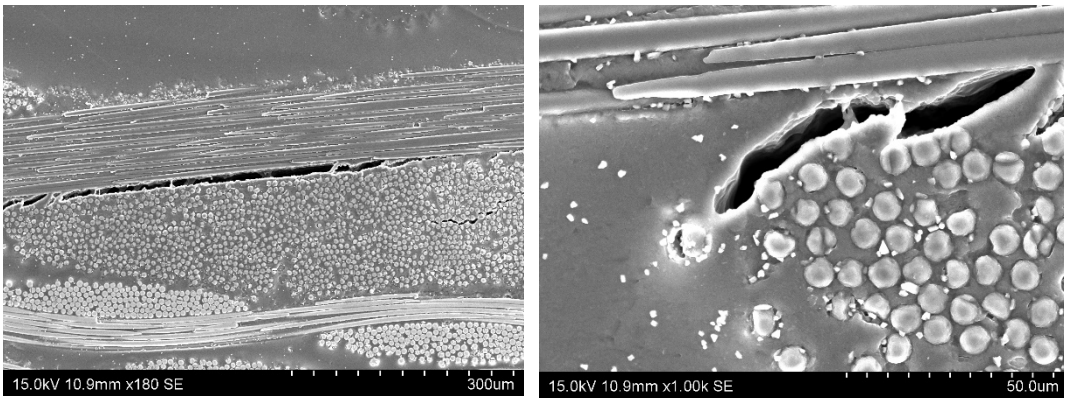

(c) (d)

Figure 6: SEM images of transversal sections of (a) LY-GNP-WCF, (b) LY-WCF, (c) and (d) LY-PEGDGE-GNP-WCF specimens (circular spots correspond to individual carbon fibers).

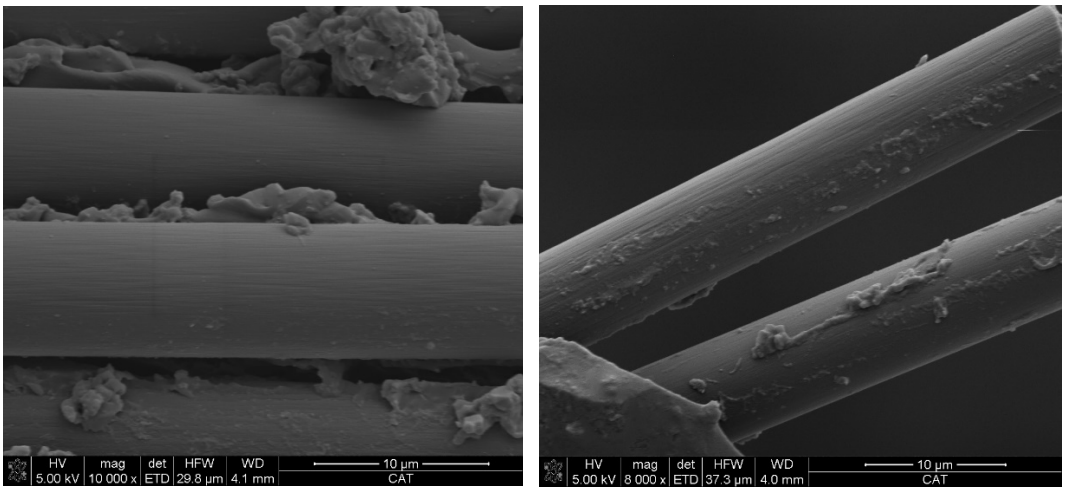

(a) (b)

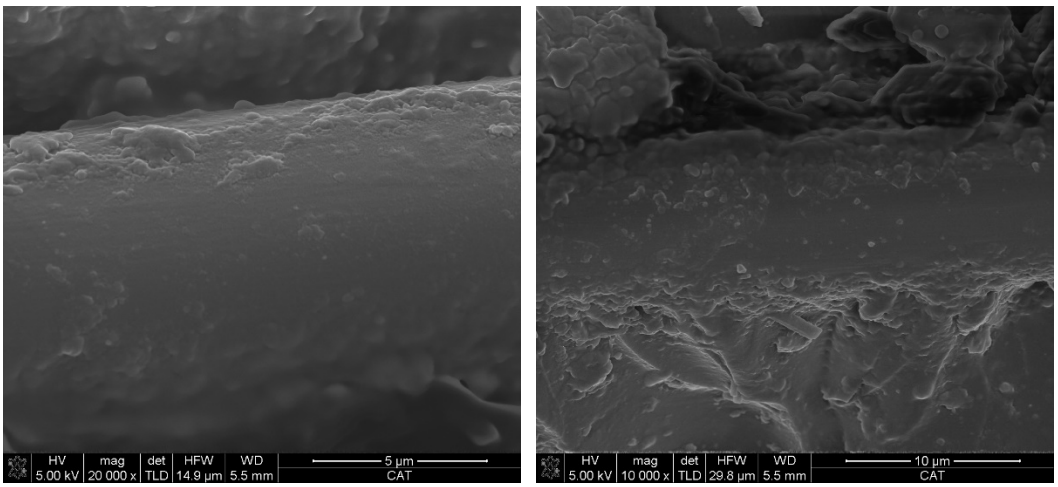

(c) (d)

Figure 7: FEG-SEM images of a fracture surface of GNP-WCF of (a), (b) LY-PEGDGE-IL and (c) and (d) neat LY resin.

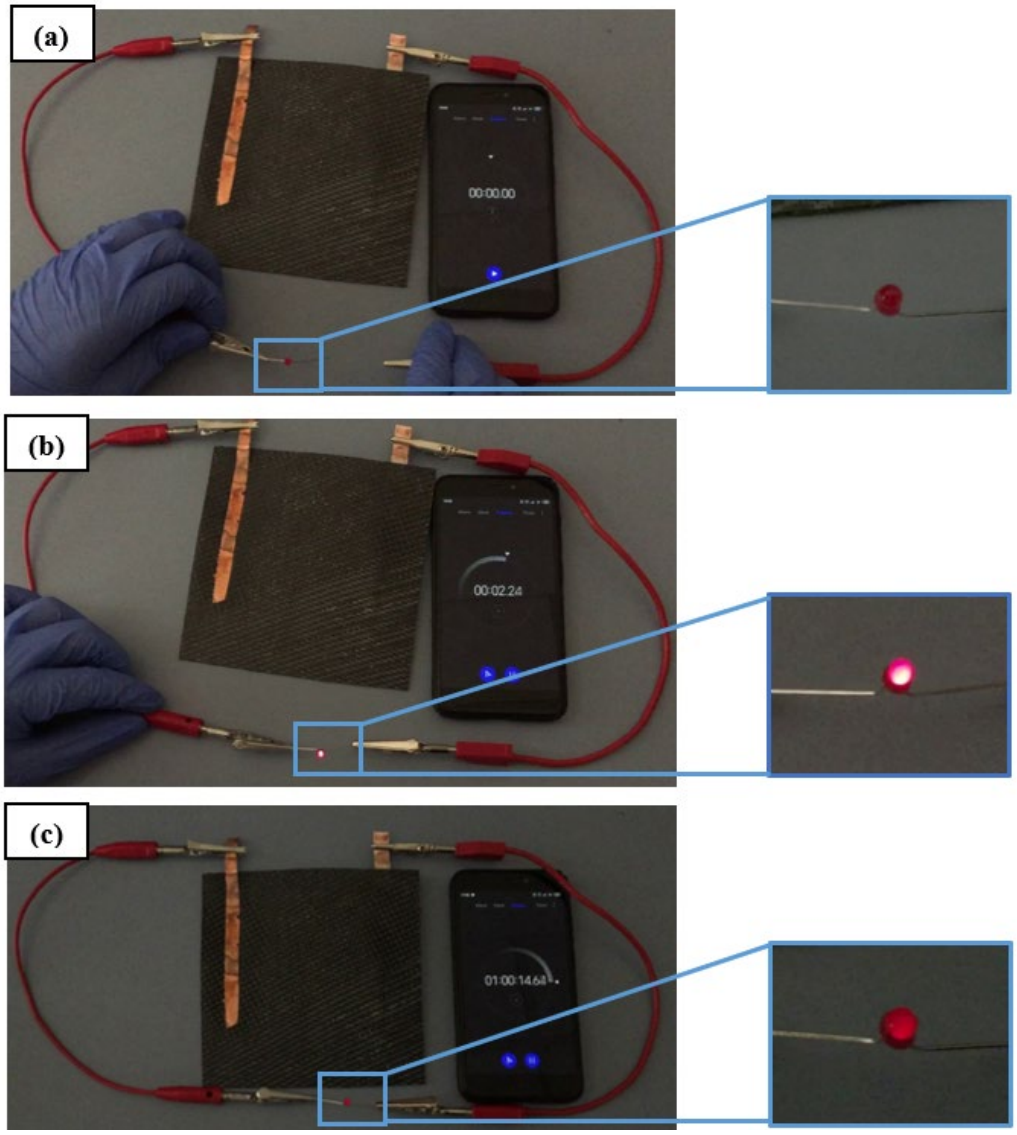

Figure 8: Proof of concept of multifunctional supercapacitor (LY-PEGDGE-IL-GNP-WCF) by illuminating a LED showing (a) the LED disconnected, (b) the LED initially illuminated (2 min after disconnection of supercapacitor from the battery) with a high luminescence and (c) the LED illuminated after 1 hour of test.